Polymer Bulletin
https://doi.org/10.1007/s00289-021-03736-4

ORIGINAL PAPER

Enhanced mechanical properties and flame retardant of epoxy resin by using of GOPOS decorated MWCNTs

Cuong Manh Vu[1] · **Huong Vu Thi**[2,3]

Received: 16 March 2020 / Revised: 17 May 2020 / Accepted: 18 May 2021

Abstract

In this study, the multi-wall carbon nanotubes (MWCNTs) were grafted with Octa (propyl glycidyl ether) polyhedral oligomeric silsesquioxane (GOPOS) to form GOPOS-G-MWCNTs prior to use as an additive for improving the mechanical and the flame-retardant characteristics of the epoxy resin (EP). The surface of MWCNTs was also modified with a silane coupling agent before conducting the grafting reaction. The Fourier-transform infrared spectroscopy technique was applied to confirm the success of the grafting reaction. The epoxy-based composite materials were performed at room temperature using diethylenetriamine (DETA) as a hardener. Many characteristics of these materials were examined such as tensile strength, thermal stability, flammability, and fracture surface morphology. The presence of GOPOS-G-MWCNTs helped to reduce the total heat release, the peak of heat release rate (pHRR), and total smoke release by 68.68, 47.69, and 11.78%, respectively. While the tensile strength and fracture energy were also increased up to 30 and 102% when compared with virgin EP. The good dispersion of GOPOS-G-MWCNTs and char residue effect were considered as the main reasons for these improvements. A mechanism for enhancing flame-retardant behaviors of EP was also proposed .

Keywords Silane compound · Mwcnts · Epoxy resin · Mechanical properties · Flame retardant

✉ Cuong Manh Vu
cuongvm@lqdtu.edu.vn; vumanhcuong309@gmail.com

[1] Faculty of Physical-Chemical Engineering, Le Qui Don Technical University, 236 Hoang Quoc Viet, Hanoi 100000, Vietnam

[2] AQP Pharma, Ha Noi, Vietnam

[3] Case Western Reserve University, Cleveland, OH, USA

Published online: 27 May 2021

Introduction

EPs have been famously utilized in many fields of industrial and engineering including automotive, composite material, coating and paints, aerospace, and electric [1–3]. However, the low flame retardant of these resins limited their application in the field required high flame retardant. The use of non-halogen additives for enhancing of the flame retardant of EP has caught the attention of many researchers as a result of environmental effects. The applying of nanomaterials for improvement of the flame-retardant characteristics of polymer matrices was also considered as a revolutionary approach [4–7]. The dispersion state of these materials in polymeric matrices can induce the effect on the properties of the matrix as mechanical and flame retardants properties [8]. With high electrical, heat, mechanical characteristics, the graphene was used as effective reinforcement to obtain the high-performance polymeric composites [9]. This material also helps to reduce the flammability of polymeric matrices because of its ability in the prevention of the gas volatiles [9, 10]. Anyway, this material hardly formed the uniform state in polymeric matrices and needed to modify its surface for further application [11]. With the structure as similar to graphene along with many active functional groups, the graphene oxide was also widely studied. The scattering of MWCNTs in epoxy matrices can be improved via the chemical surface modification of MWCNTs [12]. Cube-octameric frameworks structured GOPOS with high reactive functional groups can participate in chemical modification reaction with MWCNTs [13]. Moreover, the combustion of GOPOS can induce the thickening layer of silica char residue and can protect the surface of composite from the flame. This means that the GOPOS has its flame-retardant characteristics. Several papers reported the use of GOPOS and its hybrid materials on improvement of the flame retardant of polymer-based composite materials [14–16]. Also to the presence of an oxirane group located in the corner, the GOPOS can be easily dispersed in epoxy resin. The work related to the using of GOPOS jointing MWCNTs as a flame retardant in polymeric matrices seems to be new.

In the present study, the surface of MWCNTs has modified with an N-[3-(Trimethoxysilyl)propyl]ethylenediamine (NTPE) silane coupling agent. The nucleophilic reaction between the amine and oxirane group was considered as the main reason for strong chemical covalent linkage between GOPOS and MWCNTs. The GOPOS-grafted MWCNTs (GGOPOS-G-MWCNTs) were applied as an additive for the modification of epoxy resin. The GGOPOS-G-MWCNTs exhibited active reinforcement for EP with simultaneous enhancing mechanical and flame-retardant behaviors. A flame-retardant mechanism was also proposed for the expression the flame-retardant results.

Experimental section

Materials

Hydrogen peroxide (H_2O_2, 30%), sulfuric acid (H_2SO_4), potassium permanganate ($KMnO_4$), sodium nitrate ($NaNO_3$), hydrochloric acid (HCl, 36%), and

3-(2-Aminoethylamino)propyldimethoxymethylsilane were supplied by Sigma-Aldrich (Vietnam). MWCNTs were received from Aladdin Reagent Co., Ltd. (China). The bisphenol A-based epoxy resin (DER31) and diethylenetriamine (DETA) curing agent were supplied by Dow Chemical (Singapore). GOPOS was purchased from Hybrid Plastics Incorporation (USA).

Oxidation and silanization processing of MWCNTs

First of all, MWCNTs (2 g), and $NaNO_3$ (1 g) were charged into a 500 mL glass flask contained 60 mL of concentrated H_2SO_4. The homogeneous mixture was obtained with the help of a magnetic stirrer before cooling to zero temperature. After that, the mixture was continuously stirred for half of hour before adding of the $KMnO_4$ (10 g) for one hour along with kept the temperature below 10 ºC. The mixture was then kept in a warm water bath at 35 ºC for 5 h. After that, the temperature was risen to 90 ºC, while 120 mL of distilled water was slowly added for another 10 min along with stirring. Then, 30% H_2O_2 solution was quickly added and stirred for 10 min before simultaneous adding of both 400 mL distilled water and 175 mL of 2 wt.% HCl solution. The product was precipitated and washed again with distilled water until reached pH = 7. The aqueous suspension of oxidized MWCNTS was obtained with the help of ultrasonication technique.

The aqueous suspension of oxidized MWCNTs was used to prepare the silanized MWCNTs (s-MWCNTs) as follow processing: About 60 mL of a suspension of oxidized MWCNTs was ultrasonicated in a 500 mL glass flask with 400 mL of distilled water for 1.5 h. Then, about 6 g of silane coupling agent was added and stirred at 50 ºC for 1 day before separating with the help of filtration. The excess of silane coupling agent was removed by washing with a mixture of ethanol and distilled water (1/1 volume ratio). Finally, all excess water in product was removed by using a vacuum oven at 45 ºC for 3.5 h. The detail of oxidation and silanization processing is presented in Fig. 1 follow [17]:

Synthesis of MWCNTs grafted with GOPOS (GOPOS-G-MWCNTs)

The GOPOS-G-MWCNTs was synthesized via ring-opening reaction between amine groups located in s-MWCNTs and oxirane groups located in the surface of GOPOS. Firstly, about 6.2 g of GOPOS was stirred with 60 mL of DMF in a 500 mL glass flask by using sonication equipment for 20 min. In separate way, about 1 g of s-MWCNTs was also well mixed in 150 mL of DMF solvent before slowly adding into the mixture above for 1 h. The reaction was conducted in inner media at 120 °C with refluxing processing for a half day. In the final step, the mixture was filtered and washed with distilled water several times before drying in a lyophilizer. The detail of the grafting reaction is also presented in Fig. 1 [18]. The yield of a final product was about 86.2%.

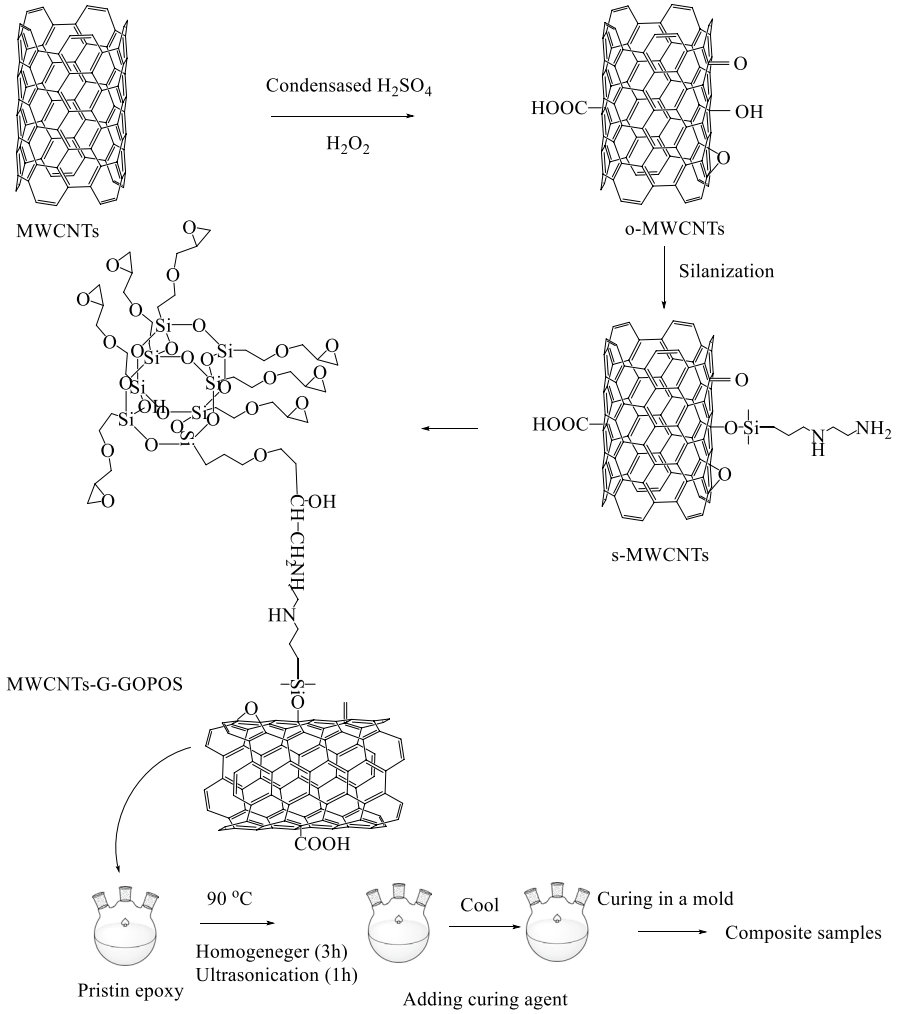

Fig. 1 Detail fabrication processing of o-MWCNTs, s-MWCNTs, GOPOS-G-MWCNTs, and epoxy nanocomposites

Preparation of epoxy composite materials

The epoxy composite materials were prepared with various contents of GOPOS-G-MWCNTs in epoxy matrix via a room curing processing. Firstly, the GOPOS-G-MWCNTs (0.2, 0.4, 0.6 wt.%) are well mixed in epoxy resin at 90 °C using a homogenizer machine for 3 h and ultrasonication for another 1 h. The mixture was then cooled to ambient condition before carefully stirring with a curing agent (10 wt.% according to epoxy weight). These mixtures were poured into a silicone mold. The curing reaction was performed at room temperature for two days. The analog procedure was also applied to prepare the epoxy sample with 0.2 wt.% of

MWCNTs for comparison aim [19, 20]. The details of this processing and chemical composition are also presented in both Fig. 1 and Table 1.

Characterization methods

The chemical structure was examined in a Fourier transform infrared (FT-IR) spectroscopy with wave number varied in the range of 400–4000 cm^{-1} and a resolution of 1 cm^{-1}.

The energy-dispersive X-ray spectroscopy (EDS) technique was used to confirm the chemical composition.

The glass transition temperature (Tg) was investigated in differential scanning calorimeter (DSC-8000 PerkinElmer, USA).

The curing level (%) was determined by the soxhlet technique. About 0.2 g of cured epoxy sample was well ground and wrapped with filter paper (m). The filter paper must be soxhlet with acetone and dried in laboratory oven until constant weight before using for wrafting with cured epoxy sample (m0). The pack of the cured epoxy sample in filter paper was extracted with acetone solvent at 80 ºC for 4 h. The samples were collected and dried again in the laboratory oven until they reached the constant weight (m1). The curing level was obtained from the following equation:

$$curinglevel = \frac{m1 - m0}{m - m0} \times 100\ (\%)$$

The flexural properties were examined in accordance with ASTM D790-86 using a universal testing machine (Instron model 5582-100KN).

The morphologies were performed in a scanning electron microscopy (SEM, Jeol JSM 6360, Japan).

The combustion characteristics of the cured samples were investigated using a cone calorimeter (Fire Testing Technology, UK) according to ISO 5660 at a heat flux of 50 kW/m^2.

Table 1 The detail component of various cured epoxy samples

Sample code	Epoxy (g)	MWCNTs (g)	GOPOS-G-GMWCNTs (g)	DETA (g)	Curing level (%)
M0	100	–	–	11.1	99.61
M1	100	0.2226	–	11.1	99.83
M2	100	–	0.2226	11.1	99.52
M3	100	–	0.4462	11.1	99.74
M4	100	–	0.6706	11.1	99.62

Results and discussion

The FTIR spectra of MWCNTs, o-MWCNTs, s-MWCNTs, and GOPOS-G-MWCNTs were examined and compared as shown in Fig. 2.

The pristine MWCNTs were characterized by the peaks at 1636 and 1406 cm^{-1} corresponded to the stretching vibration of C=C and deformation vibration of C-H in the structure of MWCNTs [21]. The oxidizing processing help to induce the oxygen functional groups into the MWCNTs surface as seen in Fig. 1 and confirm from Fig. 2. The FTIR spectrum of o-MWCNTs appeared new peaks at 3426, 1388, 1746 cm^{-1} assigned for hydroxyl group, C–O bonds of oxirane ring, and C=O bond of carbonyl group in comparison with the FTIR spectrum of virgin MWCNTs [22].

The silane coupling agent was linked with MWCNTs' surface via the condensed reaction between the OH functional groups existed in the surface of o-MWCNTs and OH formed from the hydrolysis of the silane compound as seen in Fig. 1. The FTIR spectrum of s-MWCNTs also appeared new peaks at 2930, 2862 cm^{-1} related to alkyl C–H bonds on alkyl groups of silane compound when compared with both FTIR spectra of pristine MWCNTs and o-MWCNTs. Moreover, the peaks at 1589, 1096, 1030, and 756 cm^{-1} were assigned for the N–H bonds, Si–O-Si linkage, Si–O-C linkage, and Si–C bonds. Especially, the strength of peak at 3426 cm^{-1} of OH

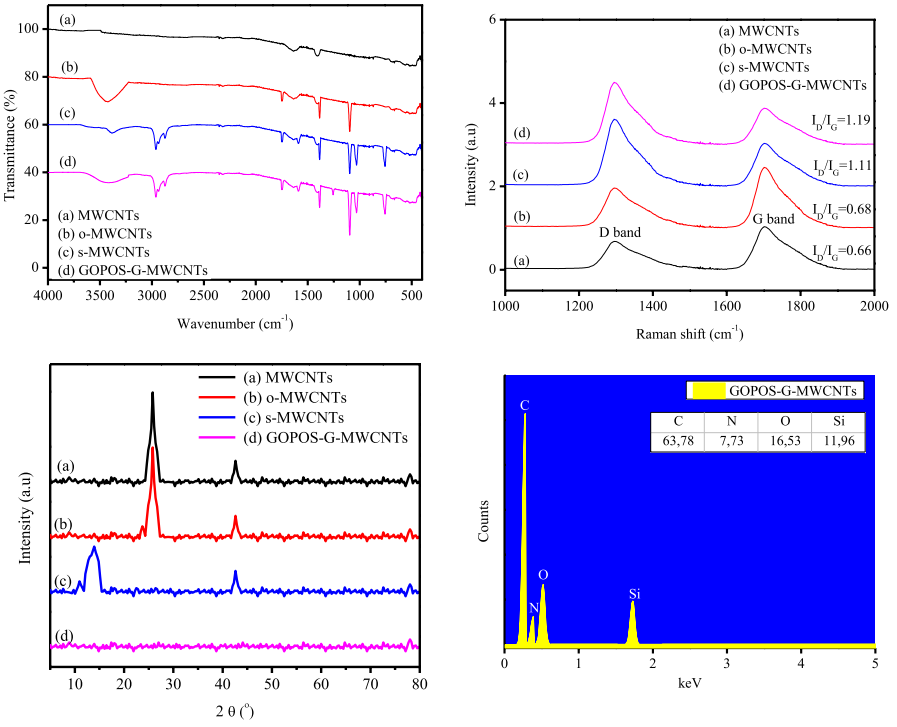

Fig. 2 FTIR, XRD, Raman spectra of MWCNT, o-MWCNTs, s-MWCNTs, GOPOS-G-MWCNTs, and EDX spectrum of GOPOS-G-MWCNTs

group was reduced. The main peaks characterized for MWCNTs still remained. The GOPOS-G-MWCNTs was synthesized from the reaction between GOPOS and s-MWCNTs via ring-opening reaction of the oxirane group located in GOPOS and amine group located in o-MWCNTs. The peak of OH group in the FTIR spectrum of GOPOS-G-MWCNTs was stronger than that OH group in s-MWCNTs as a result of ring-opening reaction. The reaction between the oxirane and amine groups induced the appearance of OH groups. The new peak was realized at 1258 cm^{-1} and was assigned for remained oxirane ring in GOPOS molecular. Moreover, the peak intensity of Si–O-Si at 1096 cm^{-1} in the FTIR spectrum of GOPOS-G-MWCNTs was increased in comparison with the peak intensity of Si–O-Si in the FTIR spectrum of s-MWCNTs. These results mean that the grafting reaction of MWCNTs and GOPOS was successfully performed [14].

The XRD technique was applied to evaluate the crystal phase of MWCNTs and its modification state as seen in Fig. 2 also. The XRD spectra of MWCNTs and o-MWCNTs were observed with no difference with peaks at 25.6 and 42.6 degrees assigned for (002) plane in hexagonal graphite [23]. However, the silanization processing induced the shifting of the peak at 25.6 degrees to 13.6 degrees along with the reducing peak intensity by comparison with the XRD spectra of o-MWCNTs and s-MWCNTs. The peaks in MWCNTs were disappeared by grafting reaction of GOPOS in the surface of s-MWCNTs due to the restraining in the recombination of MWCNTs. This means that the GOPOS molecule induced the disappearance of the crystal structure of MWCNTs. The structure of MWCNTs, o-MWCNTs, s-MWCNTs, and GOPOS-G-MWCNTs was also continuously studied with the help of Raman spectroscopy as seen in Fig. 2 also. Fig. 2 indicated that the Raman spectra of MWCNTs, o-MWCNTs, s-MWCNTs, and GOPOS-G-MWCNTs appeared two peaks in the range 1293 to 1298 cm^{-1} assigned for D band, and in the range from 1699 to 1706 cm^{-1} assigned for G band. The D band corresponded to the sp^3 carbons in graphite structure and the G band corresponded to the sp^2 carbon in the aromatic domain. The intensity of the D and G band was not affected by oxidizing processing by comparison with the Raman spectra of pristine MWCNTs and o-MWCNTs. While the intensity of the D band of s-MWCNTs and GOPOS-G-MWCNTs was improved in comparison with both D band of pristine MWCNTs and o-MWCNTs. The ratio between the intensity of D band and G band (I_D/I_G) was also calculated as seen in Fig. 2. This ratio for GOPOS-G-MWCNTs was the highest value due to the presence of both the alkyl chain of silane compound and the side chains of GOPOS [24]. While this ratio was nearly same value for both pristine MWCNTs and o-MWCNTs. The chemical compositions of GOPOS-G-MWCNTs and their weight content were also tested and showed in Fig. 2. There are four main components of GOPOS-G-MWCNTs including C, N, O, Si with the Si content about 11.96%.

The morphology of pristine MWCNTs, o-MWCNTs, s-MWCNTs, and GOPOS-G-MWCNTs is shown in Fig. 3. The results in Fig. 3 pointed out that all the type of MWCNTs have their fiber structure (as seen in SEM) and tube structure (as seen in TEM). The pristine MWCNTs (Fig. 3-A) exhibited its smooth surface with forming of agglomerate structure with the diameter about 50 nm. The thickness of the MWCNTs tube was about 2 nm as seen in Fig. 3E. The uneven of pristine MWCNTs can induce the formation of agglomerate dispersion in the epoxy composite. The

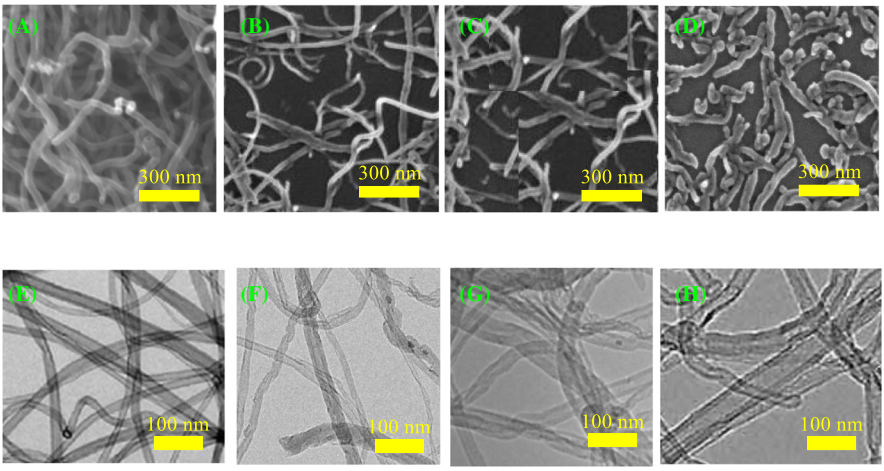

Fig. 3 SEM and TEM images of MWCNT, o-MWCNTs, s-MWCNTs, and GOPOS-G-MWCNTs

oxidation processing seemly helped to separate the fiber from the matrix as shown in Fig. 3 B. There was no extreme changing in diameter of MWCNTs after oxidizing processing. The morphology of s-MWCNTs was also more flexible than that of both pristine MWCNTs and o-MWCNTs as a result of the presence of silane molecule in its surface. The surface of GOPOS-G-MWCNTs was rough with a higher diameter (Fig. 3 D, G). The cages of GOPOS induced the change in crystal phase structure of MWCNTs by either preventing the recombination of MWCNTs or improving structural distortion. The pristine MWCNTs and GOPOS-G-MWCNTs were used as additives for fabrication of the epoxy-based nanocomposite with weight content up to 0.6 wt.% based on the epoxy resin weight. The Tg was studied from DSC results as seen in Fig. 4.

The value of Tg was normally relating to the maximum temperature of epoxy resin that can use. Figure 4 pointed out that all the curves were one step of transition without of appearance of any peaks in the tested temperature range. This means that all the samples were totally cured. The curing level (%) of all epoxy samples was nearly 100% as seen in Table 1 above. The pristine cured epoxy resin (M0) showed its Tg value of 180.1 °C. By adding 0.2 wt.% of MWCNTs (M1), the Tg value increased to 182.3 °C as a result of the limitation of segment free movement of epoxy chains. At the same content as the M1 sample, the M2 sample with 0.2 wt.% of GOPOS-G-MWCNTs presented its slightly increasing Tg value of 184.4 °C. The Tg value was continuously increasing with increasing of GOPOS-G-MWCNTs content up to 0.4 wt.% (186.8 °C) before showing the decreasing trend at a larger amount of GOPOS-G-MWCNTs content at 0.6 wt.% (185.6 °C). The GOPOS-G-MWCNTs with oxirane groups in its surface helped to improve both the dispersion and interfacial interaction between MWCNTs and epoxy chains. So that the mobility of epoxy chains was restricted as a result of enhancing the thermal stability of epoxy resin. However, when the weight content of GOPOS-G-MWCNTs increased to 0.6 wt.%, the curing agent may be not enough for both epoxy resin and oxirane groups

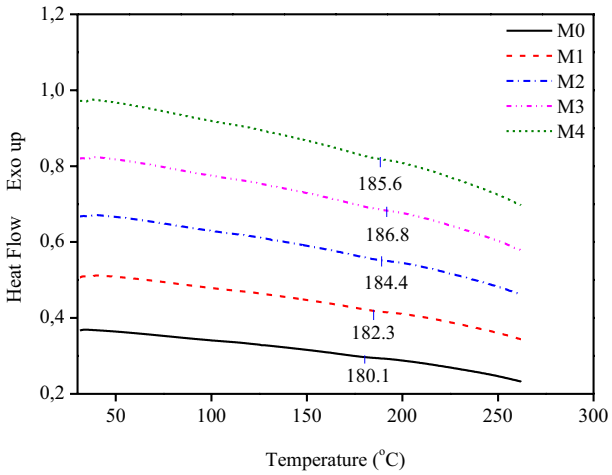

Fig. 4 DSC of various cured epoxy samples

in GOPOS-G-MWCNTs and induced incomplete cured state of epoxy resin. Moreover, the free space of cages in GOPOS can trap the epoxy resin which hardly obtains the completed cure state. In this case, the Tg would be decreased.

The flexural properties of epoxy nanocomposites were investigated, and their typical flexural stress versus flexural strain is presented in Fig. 5 follow:

The flexural strength values are also displayed in Fig. 5. As shown in Fig. 5, all the samples reached the maximum value of flexural strength before broken. The maximum flexural strength was recorded before giving the average flexural strength values. The flexural strain at the maximum flexural strength was following the elongation at break. While the hardness of nanocomposite can be relatively evaluated via the slope of stress–strain curves. The cured pristine EP sample presented its brittle characteristic. The presence of 0.2 wt.% of MWCNTs in the M1 sample the flexural strength of epoxy was reduced by 58.19%. The reduction in flexural strength may come from the bad interfacial interaction between pristine MWCNTs and epoxy chains. The flexural strength of epoxy resin was improved by adding GOPOS-G-MWCNTs with weight content up to 0.4 wt.%. The M3 sample showed its highest flexural strength value with a percent improvement of about 19.58% when compared with the M0 sample. This improvement was due to the good dispersion and good interfacial interaction between GOPOS-G-MWCNTs and epoxy matrix. The curing agent can react with both oxirane groups on the surface of GOPOS-G-MWCNTs and epoxy resin and play as the bridges between two compounds. However, the flexural strength reduced when the GOPOS-G-MWCNTs content reached 0.6 wt.%. Figure 5 also indicated that all the sample with the number from M1 to M4 have their hardness higher than that of the M0 sample.

The fracture surface of epoxy samples was observed via the SEM technique as seen in Fig. 6. The pristine EP (M0-Fig. 6A) exhibited its brittle characteristic with smooth fracture surface. Figure 6B of the M1 sample showed the agglomerate as the reason for the initiation and propagation of a crack by applying an

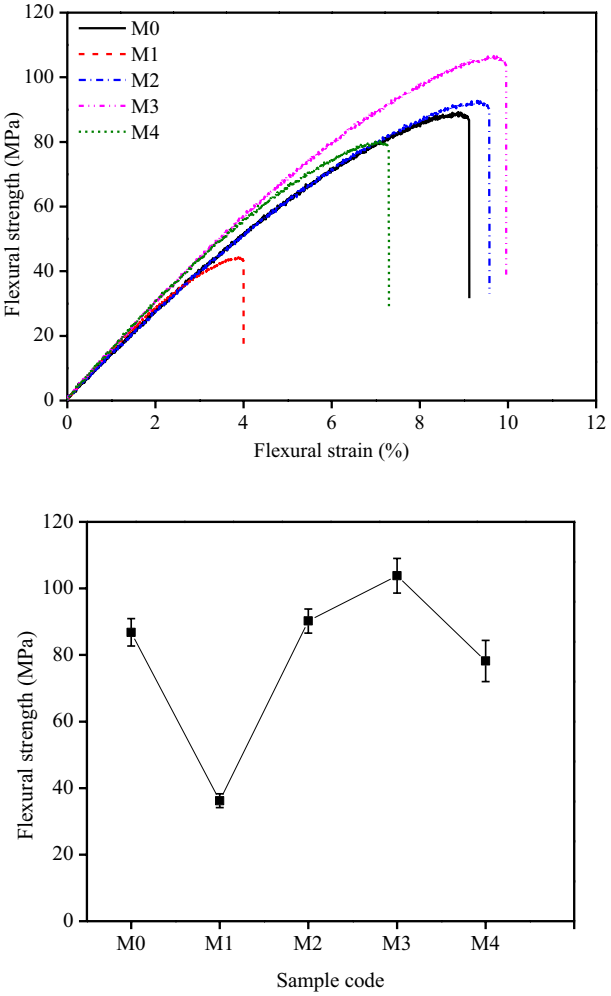

Fig. 5 Typical flexural stress–strain and flexural strength of various samples

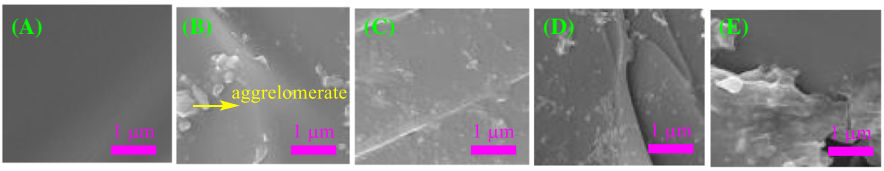

Fig. 6 Flexural broken surface of various cured epoxy samples

external force. Figure 6 C, D, E showed the good dispersion of GOPOS-G-MWCNTs in the epoxy matrix in comparison with pristine MWCNTs. The GOPOS-G-MWCNTs and epoxy matrix were stuck together as the chemical reaction

between hardener and oxirane groups in both GOPOS-G-MWCNTs and epoxy chains. This means that the crack would like to continuously propagate needed to defeat the strong covalent bonds between the GOPOS-G-MWCNTs and the epoxy matrix. The broken surface of M2, M3 corresponded to Fig. 6 C, D was rougher than that of both M0 (Fig. 6A) and M1 (Fig. 6B). The decline of flexural strength of the M4 sample was due to the breaking down the agglomeration state of GOPOS-G-MWCNTs as seen in Fig. 6 E. Generally, the presence of GOPOS-G-MWCNTs helped to improve the flexural strength of EP. These results also indicated the impact of grafting reaction of MWCNTs with GOPOS.

The flame retardant of cured epoxy samples was evaluated via cone calorimetry testing as seen in Fig. 7 and Table 2.

The HRR curves indicated that the epoxy samples showed their single peak with a decreasing trend of maximum with the presence of 0.4 wt.% of GOPOS-G-MWCNTs. While the TSR curves exhibited their increasing trend with increasing temperature before reaching the plateau region, pHHR, and TSRTHR of the M3 sample decreased about 47.69, and 68.68% when compared with the pristine sample. The reduction in pHHR was due to the crooked influence of GOPOS-G-MWCNTs in the hindrance of heat propagation. While the good chemical covalent bonds between GOPOS-G-MWCNTs and epoxy matrix formed in curing reaction were considered as the main reason for decreasing THR value. The good interaction between GOPOS-G-MWCNTs and epoxy matrix inhibited the free motion of epoxy chains. These results mean that the fire risk of burning epoxy-based materials was reduced. Moreover, the M3 sample exhibited good thermal stability with ignition time (TTI) was 56 s and higher than that of TTI value of M0 sample about 16.7%. The TGA testing also indicated that the presence of GOPOS-G-MWCNTs helped to enhance the thermal stability of EP. The char residue of the M3 sample was about 17.99% with a strong higher about 258.36% than that of the M0 sample.

Another parameter of cone calorimetry testing was total mass loss (TML) which is also presented in Table 2. The TML value related to the char influence during the combustion of cone calorimetry testing. The TML value M3 decreased by about 4.09% from 90.3 to 86.8 wt.% in comparison with the M0 sample. This means that the GOPOS-G-MWCNTs retained a larger amount of char residue in condensed phase than pure epoxy material did. The larger char layer residue indirectly suggested that not just good barrier influence also lessened the transferring of organic phase to gases.

Compared with the M0 sample, the average CO_2 yield (av-CO_2) of the M3 sample was diminished from 2.96 to 1.69 kg/kg, suggesting that the flame reaction was depressed [25].

The total smoke release (TSR) value of the M3 sample was also lower than that of the M0 sample. The reduction in TSR value means that more disintegrated fractions from the matrix were arrested in char residue [26].

The flame-retardant properties of M3 and M1 samples were compared as seen in both Fig. 7 and Table 2. The value of pHRR, THR of the M1 sample was still high in comparison with the M3 sample and near the value of the M0 sample. The char residue of the M1 sample was 7.63% and lower than 57.58% in comparison with the

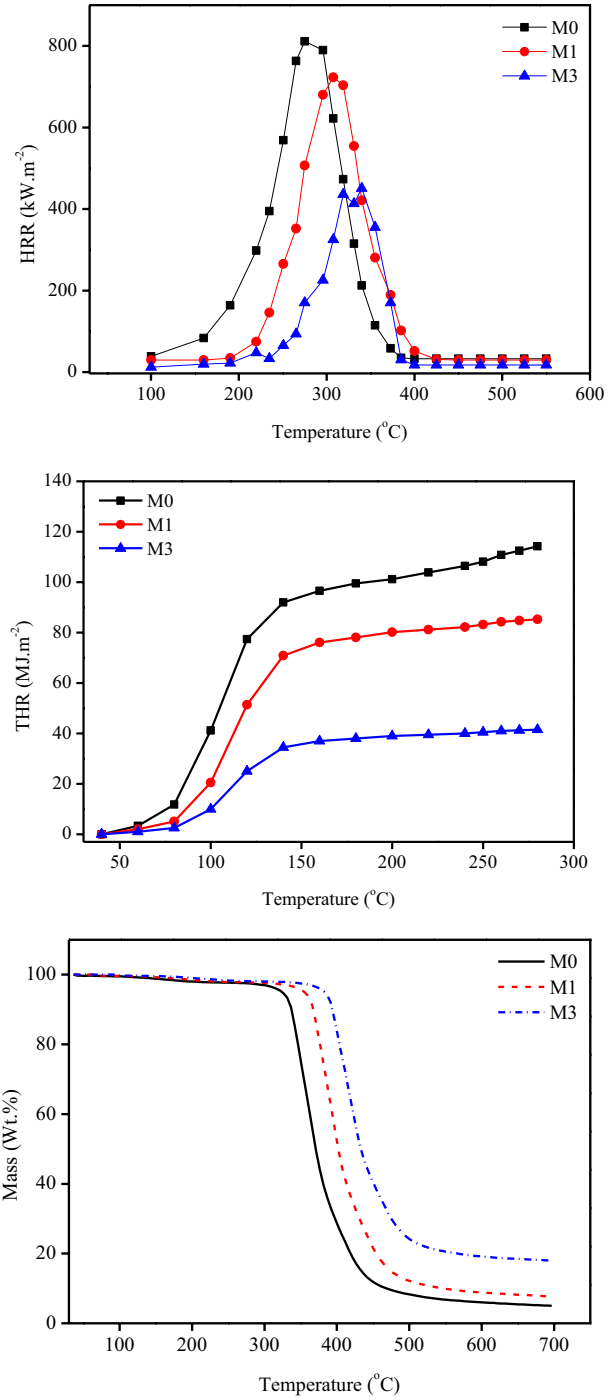

Fig. 7 HRR, TSR, PHR, and TGA curves of M0 and M3 samples

Table 2 Cone calorimetry testing results of M0 and M3 samples

Samples	pHRR ($kW•m^{-2}$)	THR ($MJ•m^{-2}$)	TTI (s)	TML (wt.%)	av-CO_2 (kg/kg)	TSR (m^2/m^2)	Char residue (%)
M0	816.28 ± 8.32	115.68 ± 3.56	48 ± 2.36	90.3 ± 3.38	2.96 ± 0.32	6028 ± 23.39	5.02 ± 0.56
M1	723.12 ± 5.68	85.28 ± 4.18	50 ± 2.14	89.2 ± 2.89	2.66 ± 0.43	5318 ± 43.26	7.63 ± 0.89
M3	426.92 ± 6.83	36.23 ± 2.12	56 ± 1.33	86.8 ± 2.89	1.69 ± 0.36	5318 ± 36.38	17.99 ± 0.98

M3 sample was the vivid evidence for the effect of GOPOS molecule located and linked in the surface of MWCNTs.

The morphology and chemical composition of char residue of epoxy samples were examined via SEM and EDS as shown in Fig. 8.

The char residue of the M0 sample showed its low flame retardant due to the presence of many holes in its surface. These hosen played a vital role in the acceleration of flame processing via easy transfer of the organic volatiles to the gas phase. The main chemical component of the char residue of the M0 sample was C and O. In opposite, the surface char residue of the M3 sample was consolidated and immovable. This layer can prevent the reaction of the condensed phase with flame as well as hindrance the diffusion of oxygen and heat into the condensed phase. This means that the flame retardant of epoxy resin was improved. The chemical component from the EDX spectrum of the M3 sample appeared a new peak of Si along with the peak of C and O. The appearance of Si indicated the formation of a firm layer in the surface of the condensed phase. The picture of char residue also indicated that the M0 sample has a thin layer of char residue. While the M3 sample exhibited the thickener layer of char residue.

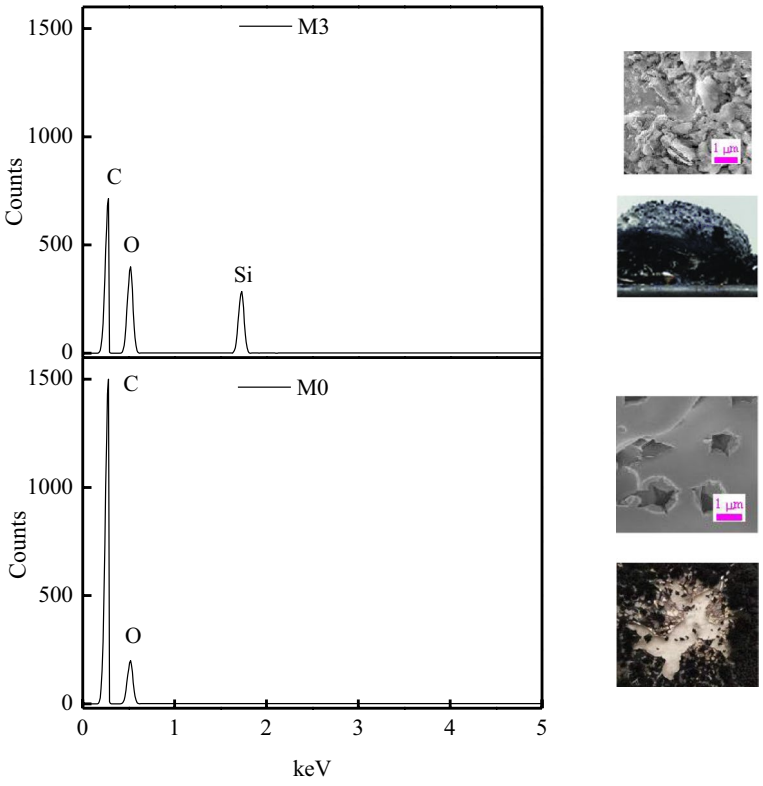

Fig. 8 SEM and chemical components of char residue of M0 and M3 samples

The main mechanisms for improvement of the flame retardant of the epoxy sample were crooked influence and formation of silicon-containing char layer in the surface of composite materials. The crooked influence was caused by the good interfacial interaction between GOPOS-G-MWCNTs and the epoxy matrix. The GOPOS-G-MWCNTs with oxirane groups on their surface can easily disperse in epoxy resin. While the huge specific area surface of MWCNTs makes the thermal path in the condensed phase became longer suggesting the prevention of the transfer between gases and heat. Moreover, the firm and an un-flammable layer of silicon-containing char residue can also prevent the contact of heat, flame, and oxygen with epoxy surface and induced the weakness of the effect of the flame.

Conclusions

In the present study, the GOPOS-G-MWCNTs was synthesized via ring-opening reaction between amine groups in silanized MWCNTs and oxirane groups in the surface of GOPOS. The chemical functional groups and morphology of synthesized GOPOS-G-MWCNTs were examined. The epoxy nanocomposites with the presence of various contents of GOPOS-G-MWCNTs were fabricated via a room curing processing using DETA as the hardener. The Tg of the epoxy matrix was slightly increased as a result of the immobility of epoxy chains at around the position of GOPOS-G-MWCNTs. The good dispersion and excellent chemical interfacial interaction between MWCNTs and epoxy chains were the main reasons for improvement both Tg and flexural strength. The epoxy sample with the presence of 0.6 wt.% of GOPOS-G-MWCNTs was recorded as a best sample with the highest improvement percent in flexural strength and flexural strain. Moreover, at this content, the THR, PHRR, and TSR were reduced by 68.78, 47.69, and 11.76% in comparison with the pristine sample. The crooked effect of GOPOS-G-MWCNTs on prolongation of the route inside EP matrix was considered as the cause of the drop in cone calorimeter properties. The thicken layer char residue formed to prevent the processing of smoke releasing was described as the main flame-retardant mechanism.

References

1. Vu CM, Nguyen DD, Sinh LH, Pham TD, Pham LT, Choi HJ (2017) Environmentally benign green composites based on epoxy resin/bacterial cellulose reinforced glass fiber: fabrication and mechanical characteristics. Polym Test 61:150–161. https://doi.org/10.1016/j.polymertesting.2017.05.013
2. Vu CM, Choi HJ, Pham TD (2017) Effect of micro/nano white bamboo fibrils on physical characteristics of epoxy resin reinforced composites. Cellulose 24:5475–5486
3. Vu CM, Nguyen DD, Sinh LH, Choi HJ, Pham TD (2018) Micro-fibril cellulose as a filler for glass fiber reinforced unsaturated polyester composites: fabrication and mechanical characteristics. Macromol Res 26:54–60
4. Liu S, Chevali VS, Xu ZG, Hui D, Wang H (2018) A review of extending performance of epoxy resins using carbon nanomaterials. Compos B 136:197–214

5. Liu S, Yan HQ, Fang ZP, Wang H (2014) Effect of graphene nanosheets on morphology, thermal stability and flame retardancy of epoxy resin. Compos Sci Technol 90:40–47
6. Zhao Y, Barrera EV (2010) Asymmmetric Diamino Functionalization of Nanotubes Assisted by BOC Protection and Their Epoxy Nanocomposites. Adv Funct Mater 20:3039–3044
7. Shao ZB, Zhang MX, Li Y, Han Y, Ren L, Deng C (2018) A novel multi-functional polymeric curing agent: Synthesis, characterization, and its epoxy resin with simultaneous excellent flame retardance and transparency. Chem Eng J 345:471–482
8. Zhang QJ, Wang YC, Bailey CG, Yuen RKK, Parkin J, Yang W, Valles C (2018) Quantifying effects of graphene nanoplatelets on slowing down combustion of epoxy composites. Compos B 146:76–87
9. Wang ZH, Wei P, Qian Y, Liu JP (2014) The synthesis of a novel graphene-based inorganic-organic hybrid flame retardant and its application in epoxy resin. Compos B-Eng 60:341–349
10. Edenharter A, Feicht P, Diar-Bakerly B, Beyer G, Breu J (2016) Superior flame retardant by combining high aspect ratio layered double hydroxide and graphene oxide. Polym 9:41–49
11. Xu WZ, Zhang BL, Wang XL, Wang GS, Ding D (2018) The flame retardancy and smoke suppression effect of a hybrid containing $CuMoO_4$ modified reduced graphene oxide/layered double hydroxide on epoxy resin. J Hazard Mater 343:364–375
12. Lee CY, Bae JH, Kim TY, Chang SH, Kim SY (2015) Using silane-functionalized graphene oxides for enhancing the interfacial bonding strength of carbon/epoxy composites. Compos A-Appl Sci Manuf 75:11–17
13. Liu HZ, Zhang W, Zheng SX (2005) Montmorillonite intercalated by ammonium of octaaminopropyl polyhedral oligomeric silsesquioxane and its nanocomposites with epoxy resin. Polym 46:157–165
14. Wang X, Song L, Yang HY, Xing WY, Kandola B, Hua Y (2012) Simultaneous reduction and surface functionalization of graphene oxide with POSS for reducing fire hazards in epoxy composites. J Mater Chem 22:22037–22043
15. Marcano DC, Kosynkin DV, Berlin JM, Sinitskii A, Sun ZZ, Slesarev A, Alemany LB, Lu W, Tour JM (2010) Improved synthesis of graphene oxide. ACS Nano 4:4806–4814
16. Bai WS, Sheng QL, Zheng JB (2016) Hydrophobic interface controlled electrochemical sensing of nitrite based on one step synthesis of polyhedral oligomeric silsesquioxane/reduced graphene oxide nanocomposite. Talanta 150:302–309
17. Qu L, Sui Y, Zhang C, Li P, Dai X, Xu B, Fang D (2020) POSS-functionalized graphene oxide hybrids with improved dispersive and smoke-suppressive properties for epoxy flame-retardant application. Eur Polym J 122:109383. https://doi.org/10.1016/j.eurpolymj.2019.109383
18. Bach Q-V, Vu CM, Vu HT, Hoang T, Dieu TV, Nguyen DD (2020) Epoxidized soybean oil grafted with CTBN as a novel toughener for improving the fracture toughness and mechanical properties of epoxy resin. Polym J 52:345–357
19. Vu CM, Nguyen VH, Bach QV (2020) Phosphorous-jointed epoxidized soybean oil and rice husk-based silica as the novel additives for improvement mechanical and flame retardant of epoxy resin. J Fire Sci 38:3–27. https://doi.org/10.1177/0734904119900990
20. Bach QV, Vu CM, Vu HT, Nguyen DD (2019) Enhancing mode I and II interlaminar fracture toughness of carbon fiber-filled epoxy-based composites using both rice husk silica and silk fibroin electrospun nanofibers. High Perform Polym 31:1195–1203. https://doi.org/10.1177/0954008319840404
21. Deyab MA, Awadallah AE (2020) Advanced anticorrosive coatings based on epoxy/functionalized multiwall carbon nanotubes composites. Prog Org Coat 139:105423
22. Mozafari V, Parsa JB (2020) Electrochemical synthesis of Pd supported on PANI-MWCNTs-SnO_2 nanocomposite as a novel catalyst towards ethanol oxidation in alkaline media. Synt Met 259:116214
23. Murugesan B, Pandiyan N, Kasinathan K, Rajaiah A, Arumuga M, Subramanian P, Sonamuthu J, Samayanan S, Arumugam VR, Marimuthu K, Yurong C, Mahalingam S (2020) Fabrication of heteroatom doped NFP-MWCNT and NFB-MWCNT nanocomposite from imidazolium ionic liquid functionalized MWCNT for antibiofilm and wound healing in Wistar rats: Synthesis, characterization, in-vitro and in-vivo studies. Mater Sci Eng C 111:110791
24. Shivakumar R, Bolker A, Tsang SH, Atar N, Verker R, Gouzman I, Hala M, Moshe N, Jones A, Grossman E, Minton TK, Teo EHT (2020) POSS enhanced 3D graphene - polyimide film for atomic oxygen endurance in low earth orbit space environment. Polym 191:122270
25. Shanglin J, Qian L, Qiu Y, Chen Y, Xin F (2019) High-efficiency flame retardant behavior of bi-DOPO compound with hydroxyl group on epoxy resin. Polym Degrad Stab 166:344–352

26. Zeng B, Liu Y, Yang L, Zheng W, Chen T, Chen G, Xu Y, Yuan C, Dai L (2017) Flame retardant epoxy resin based on organic titanate and polyhedral oligomeric silsesquioxanecontaining additives with synergistic effects. RSC Adv 7:26082